J. Fluid Mech. (2000), *vol.* 412, *pp.* 61–73. Printed in the United Kingdom

Bifurcation in a buoyant horizontal laminar jet

By JAYWANT H. ARAKERI, DEBOPAM DAS AND J. SRINIVASAN

Department of Mechanical Engineering, Indian Institute of Science, Bangalore 560 012, India

(Received 24 July 1998 and in revised form 20 September 1999)

The trajectory of a laminar buoyant jet discharged horizontally has been studied. The experimental observations were based on the injection of pure water into a brine solution. Under certain conditions the jet has been found to undergo bifurcation. The bifurcation of the jet occurs in a limited domain of Grashof number and Reynolds number. The regions in which the bifurcation occurs has been mapped in the Reynolds number–Grashof number plane. There are three regions where bifurcation does not occur. The various mechanisms that prevent bifurcation have been proposed.

1. Introduction

Buoyant jets are encountered in many engineering situations such as discharge of effluents and maintenance of solar ponds. In solar ponds, an internal convective layer can develop within the non-convective zone of the pond. To remove the internal convective layer, a brine solution is injected into it. To inject the brine at the correct location, a precise knowledge of the jet trajectory is needed. The velocity of the brine that is injected must be kept low so that the flow is laminar. The trajectory of a laminar horizontal buoyant jet in a still fluid depends upon the discharge velocity, the jet diameter and the difference in density between the jet and the environment. In this paper we present experimental observations which indicate that a horizontal buoyant laminar jet can bifurcate.

Consider a buoyant fluid issuing horizontally into still fluid from a tube with diameter d. The jet fluid density is ρ_j, its average velocity is V_j; and the ambient fluid density is ρ_a. Both the fluids have kinematic viscosity ν. The diffusivity of the species causing the buoyancy is D. The trajectory of the buoyant jet will depend on the Reynolds number ($Re = V_j d/\nu$), Grashof number ($Gr = g(\rho_a - \rho_j)d^3/(\rho_j \nu^2)$), Schmidt number ($Sc = \nu/D$), or alternatively Prandtl number (Pr) for a heated jet, and on the initial conditions, i.e. the velocity profile at the exit of the tube. In particular, the coordinates of the jet trajectory non-dimensionalized by d will also depend only on these parameters. In the present paper we consider fresh water issuing into brine, i.e. $Sc = 740$). Thus, to first order we may neglect the dependence on Sc. That is, we assume jet fluid does not diffuse into the ambient; only the momentum does. Our experiments were performed with fully developed laminar flow at the tube exit and hence the jet profile at the inlet is same in all experiments. Therefore, the trajectory of the buoyant jet will depend on Re and Gr only. Froude number ($Fr = Re/Gr^{1/2} = V_j/[(gd(\rho_a - \rho_j)/\rho_j)^{1/2}]$), a ratio of inertia to buoyancy forces, is another useful non-dimensional parameter; thus, alternatively Fr and Re can be taken as the parameters determining the trajectory. The trajectory of an inviscid buoyant jet will depend just on Fr. During the experiment we discovered that for certain values of Re and Gr the jet was not a single entity, but split into two parts. One part –

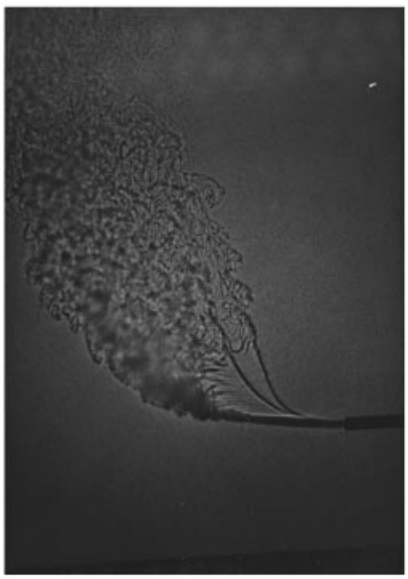

FIGURE 1. Shadowgraph picture of a typical bifurcating jet at $Gr^{1/2} = 127.4$ and $Re = 752$.

that we call the primary jet – contained the main jet fluid. The other part – that we call the plume region – was a thin sheet of the buoyant jet fluid, predominantly moving upwards. The shadowgraph of a typical bifurcating jet is shown in figure 1. In this paper, we have mapped the regions in which bifurcation occurs in the $(Re, Gr^{1/2})$-plane.

It is appropriate to mention here the scaling arrived at by Rankin *et al.* (1983) for (non-buoyant) jets starting from a parabolic velocity profile. They found that the proper non-dimensional axial coordinate is $(x/d)Re^{-1}$, where x is distance measured along the jet axis. In particular, they found that the velocity profiles reached the fully developed stage at $x/d \simeq 0.04Re$. These results should be approximately applicable to a buoyant jet in the horizontal part of its trajectory.

In § 2 we discuss the experimental technique used. In § 3 we discuss the observations. In § 4 we propose a mechanism for bifurcation. In § 5 we present our conclusion.

2. Experiments

All the experiments were conducted in a glass tank having dimensions $60 \times 30 \times 30$ cm (see figure 2). Tubes of different internal diameters (0.6, 1.4 and 3 mm) were used to discharge the jet horizontally in the tank. Each tube had a bell mouth entrance and was placed in a plenum. The tank was filled with brine of different densities. Pure water was discharged through the tube. The maximum Reynolds number was 1800. For each of the tubes, the length to diameter ratio was sufficient to ensure that the flow was fully developed and laminar at the exit. The experiment demands that the flow rate in the jet be steady and be measured accurately. In our experiment, the flow rates were too small (the maximum was about $3\,\mathrm{cm}^{-3}\,\mathrm{s}^{-1}$) to be measured by standard methods. We describe briefly the method we used which is essentially that given in Dewan, Arakeri & Srinivasan (1992) and Das (1992).

The discharge velocity was maintained steady by using a constant-head arrangement discharging across a constant resistance. The plenum was connected to a 5 l aspirator

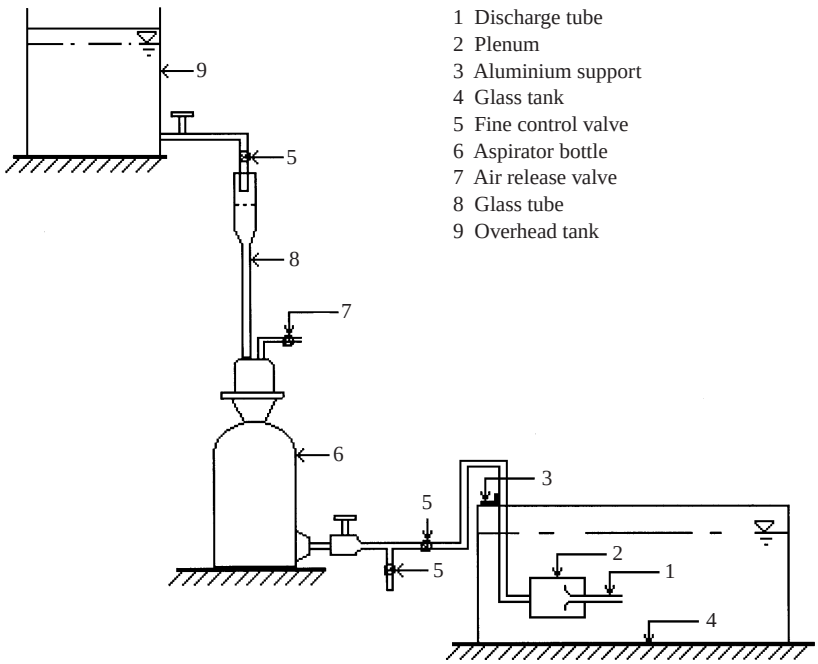

FIGURE 2. Schematic of the experimental setup.

bottle through two valves with one of them having fine control. The water level in a glass tube attached to the top of the aspirator bottle determines the head. A constant flow into the glass tube was fed from another constant-head constant-resistance arrangement. This consists of water in a large overhead tank, with a fine control valve, discharging into atmospheric pressure through a flexible tubing. Here the level in the tank provides the constant head, and the valve and the tubing the resistance. Flow rates from the overhead tank and in the jet are made equal by adjusting the position of the valve connected to the aspirator bottle such that level in the glass tube is maintained constant. Any mismatch in the flow rates is indicated by a change in level with time in the glass tube; since the tube cross-sectional area is small a small mismatch is immediately indicated. Flow rate was measured by diverting the flow from the overhead tank into a burette and measuring the time required to collect 10 ml of sample.

The Grashof number Gr was varied by using brine with different densities in the tank and using the different diameter tubes. The Reynolds number was varied by varying the flow rate as well as by using different diameter tubes. The uncertainty in the measurement of flow rate and density resulted an error in the calculation of Re, Fr and Gr within 5%, 8% and 7% respectively. The jet trajectory was visualized either by shadowgraph or using dye (potassium permanganate or fluoresceine).

3. Results

The experimental data are shown in figure 3(a) as a function of two non-dimensional parameters Re and $Gr^{1/2}$; figure 3(b) is an exploded view showing the data points of the lower part of figure 3(a). The region in the $(Re, Gr^{1/2})$-plane where the buoyant jet bifurcates is indicated by the symbol $*$ and wherever there is no bifurcation is shown

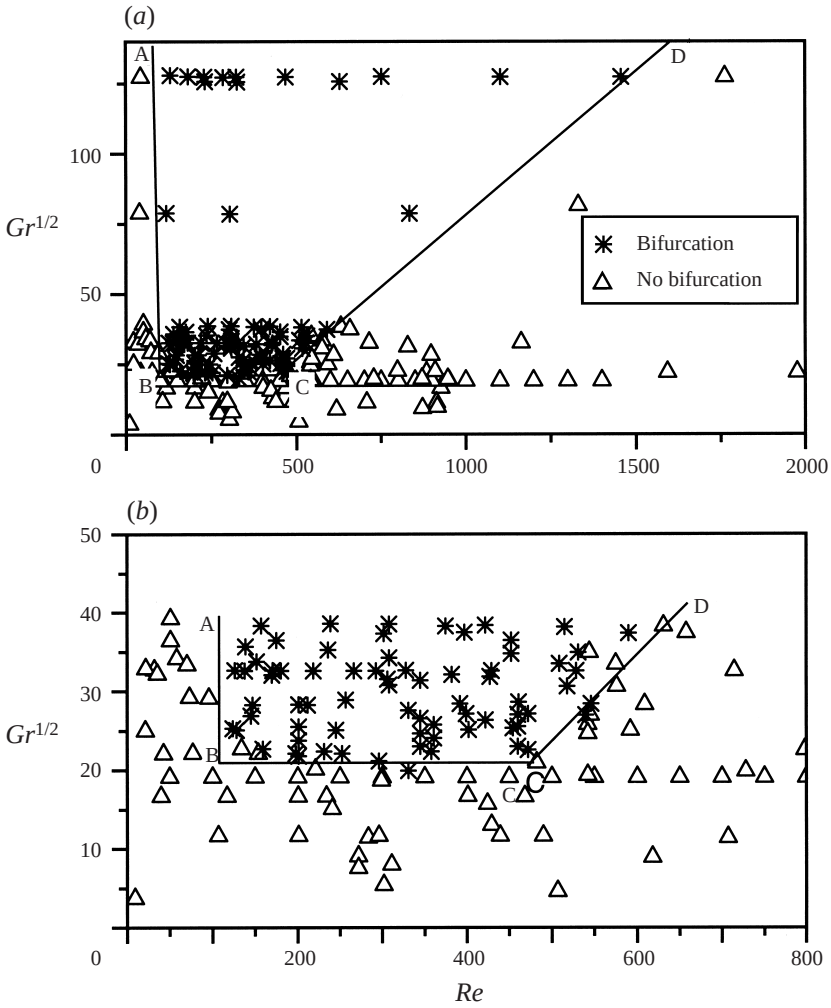

FIGURE 3. Regions of bifurcation shown in $(Re, Gr^{1/2})$-plane.

by symbol △. It is useful to draw roughly three boundary lines – AB, BC and CD. No bifurcation occurs in the regions to the left of AB (i.e. $Re < 100$), below BC (i.e. $Gr^{1/2} < 20$) and to the right of CD. The reasons why these three boundaries exist is discussed in the next section.

First we examine the various flow features at different $Gr^{1/2}$ and Re with the help of shadowgraph pictures. Figure 4 indicates the Re and $Gr^{1/2}$ values of the jets in all the shadowgraph pictures given in this paper. Also shown in figure 4 are the boundaries and lines of constant Froude number Fr. Figure 5 shows a series of shadowgraph pictures at a fixed $Gr^{1/2} = 127.4$ and Re varying from 62 to 1761. The Froude number varies from 0.49 to 13.8. Dewan *et al.* (1992) have shown that both Fr and Re have an effect on the trajectory. The effect of Fr is clear: a low-Fr (buoyancy dominating over inertia) buoyant jet will move rapidly upwards and become vertical within a short distance while a jet with a high Fr (inertia dominating over buoyancy) will have a flatter trajectory. The effect of Re comes through entrainment. A high-Re jet will have a lower entrainment and hence a flatter trajectory compared to a low-Re jet at the

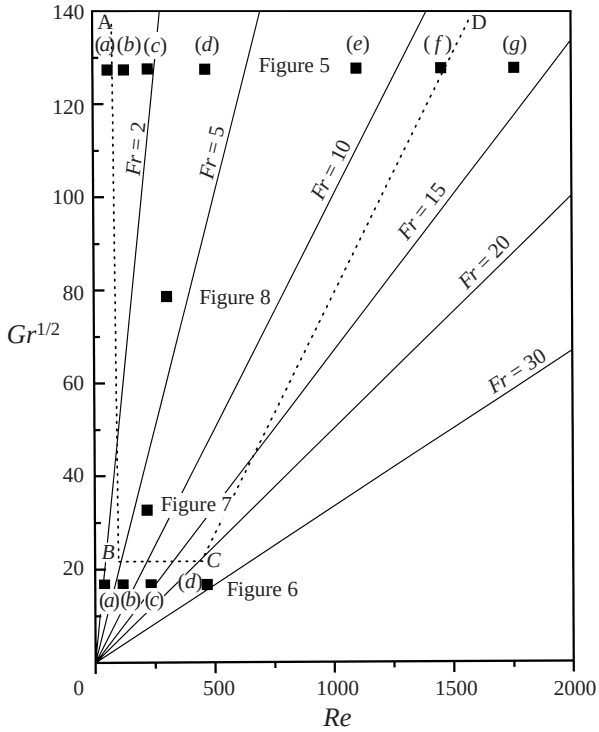

FIGURE 4. Re and $Gr^{1/2}$ values of jets shown in shadowgraph pictures along with the boundaries showing the regions of bifurcation and no bifurcation.

same Fr value. Thus, in figure 5 with both Re and Fr increasing we have trajectories which are highly curved (figure 5*a*) to flat (figure 5*f*). Besides the trajectory other changes occur in the jet when Re changes. Bifurcation is observed to occur in figure (5*b–f*). Transition to turbulence occurs both in the main jet and in the plume region.

At $Re = 62$ (figure 5*a*) we observe that the buoyant jet turns up rapidly and become nearly vertical in a short distance from exit. Transitional flow appears at a distance of approximately $10d$ along the trajectory of the jet from the exit of the tube. At $Re = 130$ (figure 5*b*) we observe that the jet bifurcates at a distance of $2d$ from the jet exit. Transition in the main jet occurs at a distance of approximately $10d$ whereas transition in the plume region occurs at a distance of approximately $15d$. A thin layer of jet fluid exists in between the main jet and the bifurcated plume. In the turbulent region the jet and the plume merge into a single jet. Similar features of the jet can be observed at $Re = 229$ and 468 (figure 5*c*, *d*). Instability waves can be seen in the thin layer of liquid between the jet and the plume in these cases. At $Re = 468$ and 1102 (figure 5*d*, *e*) two bifurcated plumes can be observed. The distance at which bifurcation occurs is always less than the distance at which transition occurs. Distance between the point of bifurcation and the point of transition decreases as the Reynolds number increases (see figure 5*b–f*). The point of bifurcation moves from about $2d$ at $Re = 130$ to about $12d$ at $Re = 1457$. At this value of $Gr^{1/2}$ (i.e. 127.4) bifurcation is not observed for Re greater than about 1700 (figure 5*g*).

Figure 6 shows shadowgraph pictures for fixed $Gr^{1/2}(= 16.7)$, and Re varying from 40 to 468 and Fr from 2.4 to 28.0. They correspond to non-bifurcating jets (i.e. points below the boundary BC). The effect of Fr is evident in the changing trajectory. The

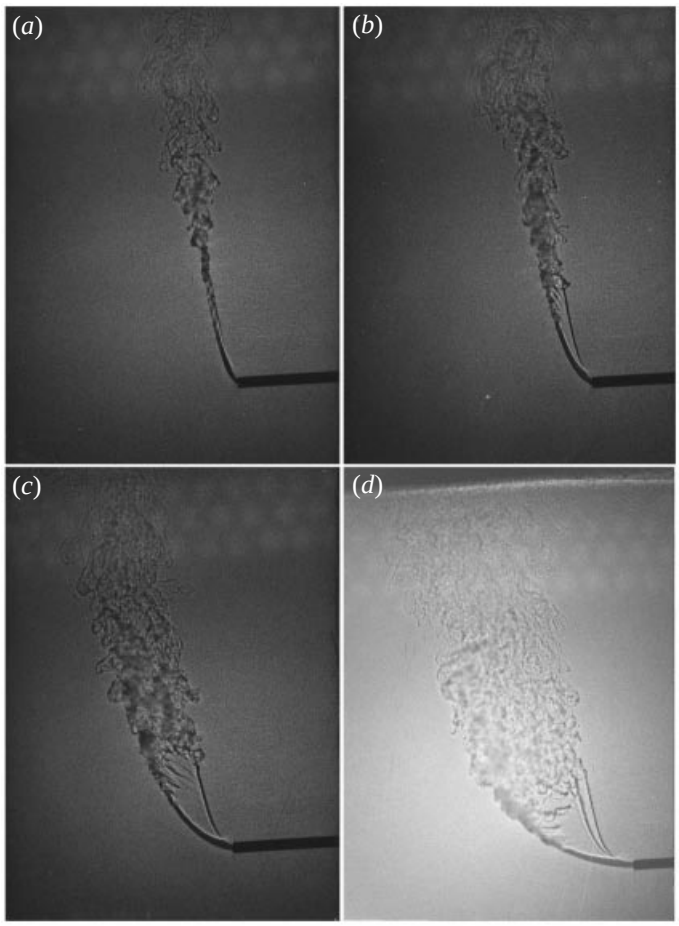

FIGURE 5. For caption see facing page.

transition length L_{tr} (the distance between the jet exit and the transition point along the trajectory of the jet) is $70d$ at $Re = 40$ (figure 6*a*, it decreases to $50d$ at $Re = 116$ (figure 6*b*) and increases with Re till about $Re = 450$ (figure 6*c*, *d*); at $Re = 468$ $L_{tr} \simeq 80d$. However L_{tr} decreases as Re increases further; at $Re = 926$, $L_{tr} \simeq 30d$ (not shown). Figure 7 shows a bifurcating jet ($Gr^{1/2} = 32.6$, $Re = 218$, $Fr = 6.7$) just above the boundary BC, and figure 8 shows a bifurcating jet at about the same Re but higher $Gr^{1/2}$.

Figure 9 shows the variation of transition length L_{tr} with Re for different values of $Gr^{1/2}$. At high $Gr^{1/2}$ (= 127 and 78) the transition length does not vary with Re. At low $Gr^{1/2}$ the variation of L_{tr} with Re is different from that of high $Gr^{1/2}$ as can be seen in figure 9. As Re increases L_{tr} initially decreases with Re. At lower Re the jet becomes vertical in a short distance and remains laminar for a long distance. As Re increases the jets become more slanted and the transition length decreases. But when the jet trajectory becomes more horizontal the transition length increases. L_{tr} decreases with Re when the jet trajectory is almost horizontal for a long distance from the exit. When $Gr^{1/2}$ is in the range 17 to 32 we observe such variations of L_{tr} with Re.

It may be remarked that very few studies on transition at moderate Re exist even for non-buoyant jets. Milojevic & Schneider (1993) have compiled data from various

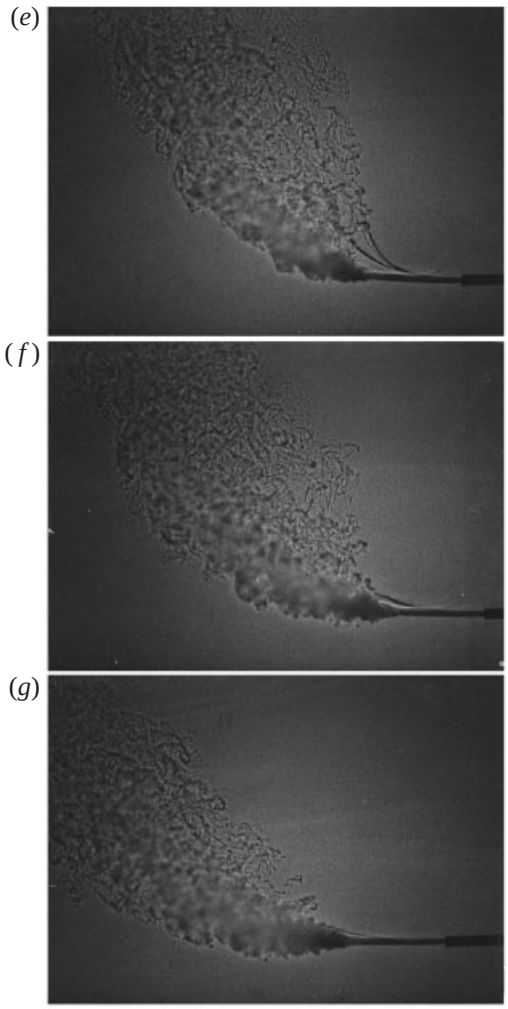

FIGURE 5. Shadowgraph pictures of jets at $Gr^{1/2} = 127.4$ and varying Re. (*a*) $Re = 62$, (*b*) $Re = 130$, (*c*) $Re = 229$, (*d*) $Re = 468$, (*e*) $Re = 1102$, (*f*) $Re = 1457$ and (*g*) $Re = 1761$.

sources on transition lengths in non buoyant jets at moderate Re. There is lot of scatter in the data; for example at $Re = 250$, L_{tr}/d varies between 100 and 700 and at $Re = 1000$, L_{tr}/d varies between 8 and 60. At the lower Gr our data for L_{tr} are consistent with those given in the above reference.

Figure 10 shows the variation of length required for the jet to bifurcate (L_b/d), measured along the direction of the trajectory of the jet with Fr. As Fr increases L_b/d increases linearly. The best-fit linear curve shows that the slope of the curve is 1.16.

4. Theory and discussion

4.1. *Theory*

In this section we propose a mechanism which can cause bifurcation. The buoyant jet may be thought of as containing three parts: the core jet fluid which constitutes the primary jet, the peripheral jet fluid which constitutes the plume, and the entrained

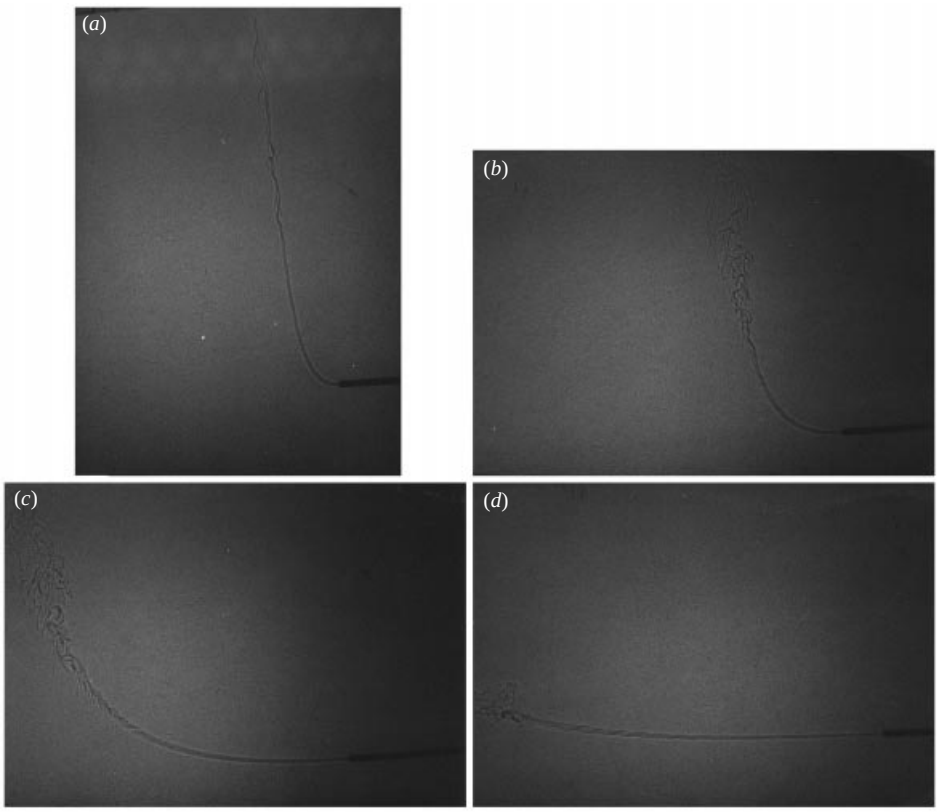

FIGURE 6. Shadowgraph pictures of jets at $Gr^{1/2} = 16.7$ and varying Re. (a) $Re = 40$, (b) $Re = 116$, (c) $Re = 234$, (d) $Re = 468$.

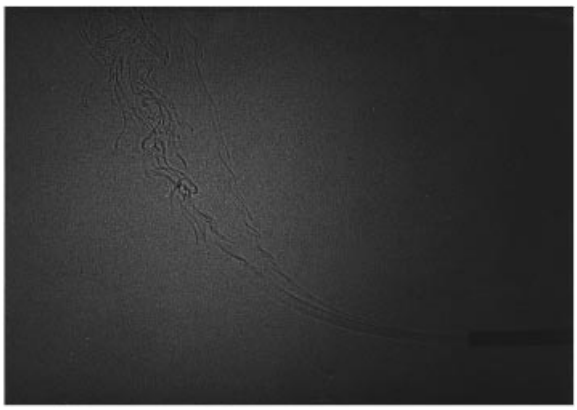

FIGURE 7. Shadowgraph picture of a bifurcating jet at $Gr^{1/2} = 32.6$, $Re = 218$.

fluid. A cross-section of the jet a short distance from the exit showing the three parts and the velocity and density distributions is given in figure 11.

Bifurcation is related to the fact that velocity varies across any cross-section of the jet. For a given density difference, fluid particles having higher velocity will have a flatter trajectory than those having lower velocity. Thus the core of the jet fluid with

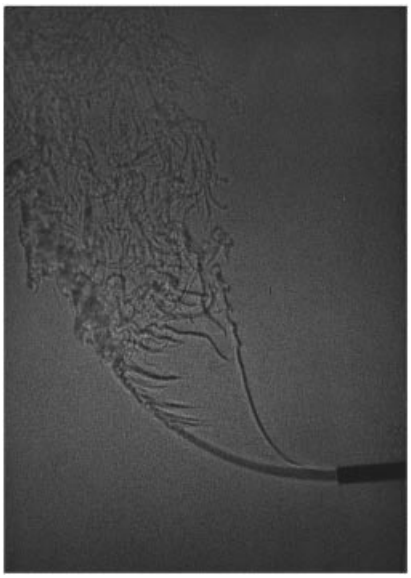

FIGURE 8. Shadowgraph picture of a bifurcating jet at $Gr^{1/2} = 78.6$, $Re = 304$.

a higher velocity has a flatter trajectory and forms the primary jet; the periphery of the jet fluid with a lower velocity forms the plume region. We verified this hypothesis by tracing the trajectories of different parts of the jet fluid by using a dye. We found that even the fluid near the bottom wall of the tube ends up in the plume. Figure 12 shows a schematic of the path taken by the peripheral fluid.

Let us consider why bifurcation does not always occur. We may consider bifurcation by looking at the vertical displacement of the peripheral fluid with respect to the core fluid. A balance of buoyancy ($\Delta\rho g/\rho$) and inertia forces ($U_s \partial v/\partial x$) gives an estimate of the vertical displacement, Δy_s, in a distance x_s:

$$\frac{\Delta y_s}{d} \simeq \frac{\Delta\rho}{\rho_j} g d \left(\frac{x_s}{d}\right)^2 \frac{1}{\overline{U_s}^2},$$

where $\Delta\rho$ is the density difference between the ambient and the jet fluids, U_s is the horizontal velocity of the peripheral fluid – the bar representing an average (average taken over x_s), and v is the vertical velocity ($\simeq U_s \, \mathrm{d}(\Delta y_s)/\mathrm{d}x_s$). We may estimate the bifurcation distance L_b by assuming that bifurcation occurs when $\Delta y_s/d \sim 1$; also we have $\overline{U_s} \sim V_j$. Thus $L_b/d \sim Fr$. Figure 10 shows that the experimental bifurcation length is nearly linearly proportional to Fr with the slope $\simeq 1.2$. Therefore we may write

$$\frac{L_b}{d} \simeq 1.2 Fr.$$

It is interesting to rewrite the above relation in terms of Re so that L_b has the non-dimensional form proposed by Rankin *et al.* (1983) for non-buoyant jets:

$$\left(\frac{L_b}{d}\right) \frac{1}{Re} = \frac{1.2}{\sqrt{Gr}}.$$

At the lowest $\sqrt{Gr}$ ($= 20$) at which we observe bifurcation we get $(L_b/d)/Re \simeq 0.06$.

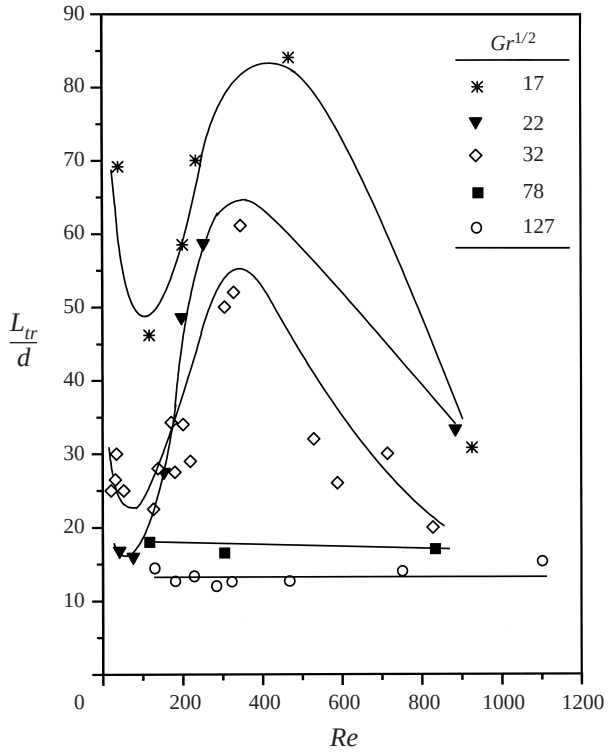

FIGURE 9. Variation of the transition length, L_{tr} with Re for different values of $Gr^{1/2}$.

Recall non-buoyant jets become fully developed at $(x/d)/Re \simeq 0.04$. Thus only at the lowest Grashof number values is the jet fully developed when bifurcation occurs.

With this background we can explain the three boundaries between bifurcation and no bifurcation in figure 3. In the region to the left of AB in figure 3 the jet turns vertical too quickly to permit bifurcation; the horizontal extent, say L_{turn}, of the jet is small. We may expect bifurcation to be prevented if $L_{turn} < L_b$. We may expect the jet to turn vertical within a short distance for low values of Fr or low Re. However, at this point we do not have any theory as to why the boundary is a constant-Re line or any explanation which gives the Re value of 100. It is surprising that the boundary AB is a line of constant Re and not constant Fr. Interaction of the peripheral buoyant fluid and the entrained non-buoyant fluid may provide one possible reason for the role played by Reynolds number. A three-dimensional numerical simulation may provide some physical insight.

In the region to the right of CD transition to turbulence occurs before bifurcation can set in. This can be seen by comparing, for example, figures 5(f) and 5(g). We have seen in figure 9 that the transition length, L_{tr}, depends on both Re and Gr in a complicated way. However, at the higher values of Gr ($Gr^{1/2} \sim 100$), $L_{tr}/d \simeq 15$. Equating L_{tr} and L_b and using $L_b \simeq 1.2Fr$ we arrive at an estimate of boundary CD as $Fr \simeq 12.5$ which is approximately consistent with figure 3. This also explains why the boundary CD is not vertical.

The boundary BC ($Gr^{1/2} < 20$) exists because viscous diffusion reduces sufficiently the difference between core fluid velocity and peripheral fluid velocity and hence prevents bifurcation. Momentum diffuses over a lateral distance d in an axial length,

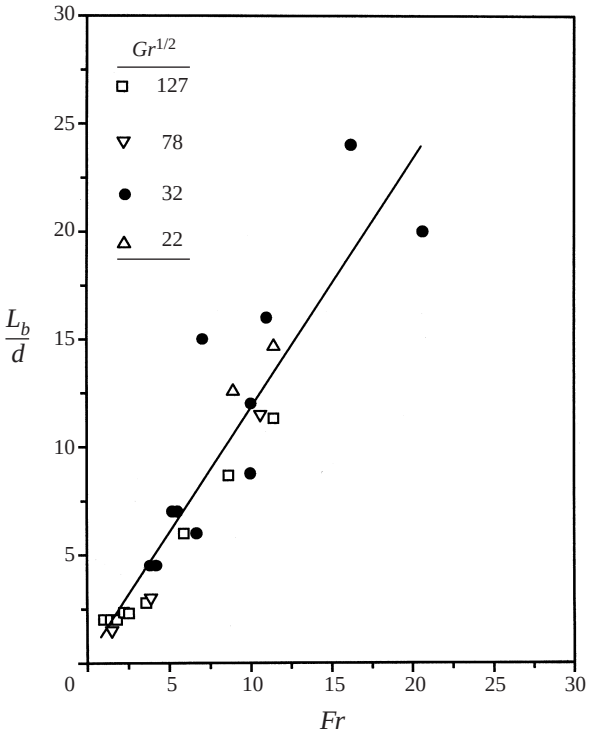

FIGURE 10. Variation of the bifurcation length, L_b/d with Fr.

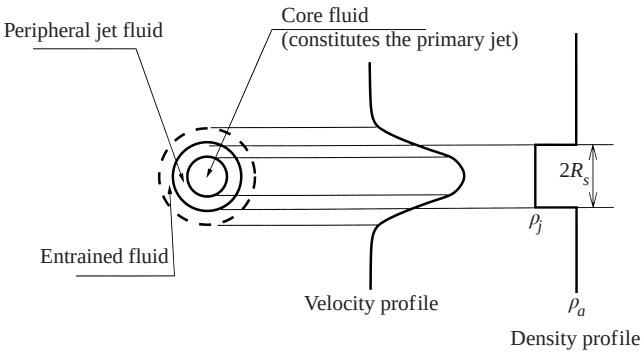

FIGURE 11. Density and velocity distributions across a cross section of a high Schmidt number jet. $2R_s$ is the diameter of the jet fluid.

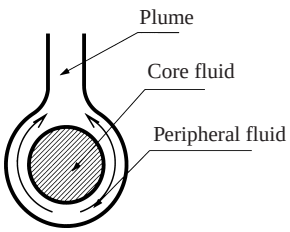

FIGURE 12. Schematic showing path taken by peripheral jet fluid, to form the plume.

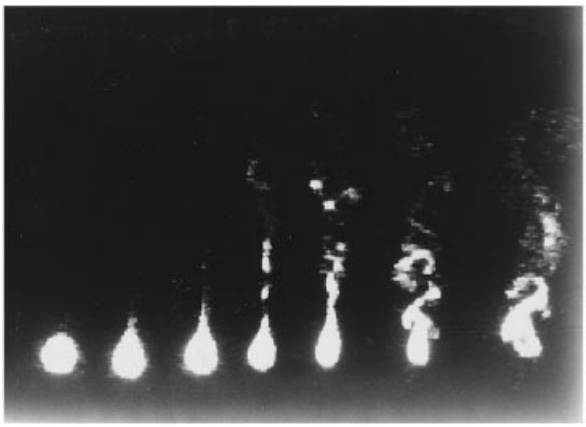

FIGURE 13. Cross sections of the jet showing the primary jet and the plume instability for $Re \simeq 350$ and $Gr^{1/2} \simeq 210$ at $x/d = 0.2, 1.2, 1.5, 2, 3, 4$ and 6.

say, $L_{diff} \sim d^2 V_j/\nu$. Bifurcation would not occur if $L_{diff}/d < L_b/d$, i.e. $k_1 Re < Fr$ or $Gr^{1/2} < 1/k_1$ where k_1 is a constant. From the experimental value of $Gr^{1/2} = 20$ we get $k_1 \simeq 0.05$.

In summary we find experimentally the bifurcation length $L_b \simeq 1.2Fr$. Bifurcation is not observed if the buoyant jet becomes vertical within a short distance (i.e. $L_{turn} < L_b$), if transition to turbulence occurs before bifurcation can (i.e. $L_{tr} < L_b$) or if sufficient viscous smoothing of the velocity profiles takes place before bifurcation (i.e. $L_{diff} < L_b$).

4.2. *Discussion*

The bifurcation process is probably nonlinear: formation of the plume is a result of imbalance of forces, and once the peripheral fluid starts separating from the primary jet it encounters fresh ambient (still) fluid and thus further loses horizontal momentum. This will accelerate the process of bifurcation.

The plume region of a bifurcating jet is essentially a sheet of fluid moving upwards due to buoyancy. The horizontal component of velocity in this region is small. The nearly horizontal lines seen in the shadowgraph pictures are due to sinuous instability, as can be clearly seen in the cross-sectional slices of the jet visualized by fluorescent dye and the laser sheet of light (figure 13). The transition to turbulence, characteristic of free shear flows, is abrupt. In most cases, transition to turbulence in the primary jet is seen to occur upstream of the transition in the plume.

Momentum diffusion causes motion in the ambient still fluid. This entrained fluid is non-buoyant. Just downstream of the buoyant jet exit both the jet fluid and the entrained fluid will move nearly horizontally. However, further downstream, the jet fluid (with or without bifurcation), will move upwards due to buoyancy whereas the entrained fluid will tend to continue to move horizontally. At each location of the buoyant jet trajectory entrainment takes place but with the entrained fluid tending to take a path different from the jet fluid. We confirmed some of these conclusions by introducing dye in the ambient and observing its motion. The nearly vertical striations in some of the shadowgraph pictures appear to be due to jet fluid being pulled to the side by the entrained fluid. Clearly, the effect of these differences in trajectories is important only near the curved regions of the jet trajectory. These considerations

apply to both laminar and turbulent buoyant jets which are non-vertical, and can have important implications in the calculation of growth rates and mixing.

So far we have considered high Schmidt number or high Prandtl number jets which are fully developed at the exit. It is relevant to ask under what other conditions bifurcation would occur. Our experiments with a sharp-edged orifice, instead of a pipe, in which case the exit velocity profile will be nearly top hat, showed bifurcation. The boundaries between bifurcation and no bifurcation were, however, different from the fully developed flow case. The momentum flux which diffuses rapidly will create a velocity gradient a short distance from the exit that will lead to conditions suitable for bifurcation.

Jets where buoyancy and momentum diffuse at the same rate (i.e. Sc (or Pr) ~ 1), are unlikely to bifurcate if the shapes of the exit profiles of velocity and concentration are same. Hence turbulent buoyant jets, with an effective Sc (or Pr) near unity do not bifurcate, as found in this study and by others (Satyanarayana & Jaluria 1982) who have investigated turbulent buoyant jets. One of the reviewers suggested that a similar type of bifurcation has been observed in inclined turbulent flame plumes (Escudier 1975). The flow however is more complex in view of the heat release due to combustion. The theories proposed here may not be applicable in such cases.

5. Conclusion

Bifurcation of a laminar water jet was observed when it issued horizontally into brine. Bifurcation was found to occur in high Schmidt (or high Prandtl) number jets and was due to the slower moving fluid at the periphery of the jet. Bifurcation does not occur at low Gr because of viscous effects. At low Re the buoyant jet turns vertical before it can bifurcate and at high Re, the jet becomes turbulent before it can bifurcate.

REFERENCES

Das, D. 1992 Study of buoyant jets discharged horizontally in stratified and uniform ambient media. Master of Engng thesis, Dept. of Mech. Engng, Indian Institute of Science, Bangalore, India.

Dewan, A., Arakeri, J. H. & Srinivasan, J. 1992 A note on high Schmidt number laminar buoyant jets discharged horizontally. *Intl Commun. Heat Mass Transfer* **19**, 721–731.

Escudier M. P. 1975 Analysis and observations of inclined turbulent flame plumes. *Combust. Sci. Technol.* **10**, 163–171.

Milojević, D. K. & Schneider, W. 1993 Free confined jets at low Reynolds numbers. *Fluid Dyn. Res.* **12**, 307–322.

Rankin, G. W., Sridhar, K., Arulraja, M. & Kumar, K. R. 1983 An experimental investigation of laminar axisymmetric submerged jets. *J. Fluid Mech.* **53**, 217–231.

Satyanarayana, S. & Jaluria, A. 1984 A study of laminar buoyant jets discharged at an inclination to the vertical buoyancy force. *Intl J. Heat Mass Transfer* **25**, 1564–1569.